



## Research article

## Design and circuit analysis of a single and dual band-notched UWB antenna using vertical stubs embedded in feedline



Mubarak Sani Ellis<sup>\*</sup>, Philip Arthur, Abdul Rahman Ahmed, Jerry John Kponyo, Benedicta Andoh-Mensah, Bob John

Department of Telecommunication Engineering, Kwame Nkrumah University of Science and Technology, Kumasi, Ghana

## ARTICLE INFO

## Keywords:

UWB antennas  
Band-notched  
WLAN  
WiMAX  
Microstrip feedline  
Circuit theory  
Band rejection  
Filtering

## ABSTRACT

Within the frequency band designated by the FCC for UWB systems, there are other frequency bands that are also designated for use for other technologies like WLAN (5.15 – 5.35 GHz) and WiMAX (3.3–3.7 GHz). These systems can cause interference with UWB systems when operated at the same time. Therefore, an antenna operating in the UWB spectrum needs to have band-notch capabilities in order to mitigate interference resulting from nearby communication systems operating within the UWB frequency band. In this paper, the notched bands are achieved by using vertical stubs protruded from a microstrip feedline. The antenna is etched on a  $25 \times 30 \text{ mm}^2$  substrate. Two antenna structures are presented; one is designed to notch an intended narrowband from 3.3 – 3.6 GHz and the second is designed to include an additional band notch from 5.15 – 6 GHz. The simulations and measurements show that the proposed antennas achieve an ultra-wide bandwidth of 3–10.6 GHz with successful single and dual band-notches, good gain and good group delay rejection in the notch bands. Stable radiation patterns with low cross polarization are also realized across the operating bandwidth. A detailed analysis of how the filtering is also achieved using circuit theory is presented in this work as well.

## 1. Introduction

Ultrawideband (UWB) systems uses high frequency radio waves for short range communications. They have become very attractive for high data rate transmission due to the advantage it has from spreading of RF energy over a very wide bandwidth. UWB systems therefore communicate with signals with low power spectral density and have an immunity against multipath effects as a result [1]. Research into UWB antennas has resurged in recent years due to the availability of low-cost but powerful computing SoCs and the need for accurate location tracking and ranging in the emerging technological landscape.

Among the numerous types of UWB antennas proposed, the planar monopole UWB antenna [2, 3] has gained the most attention due to its small size, low cost and ease of integration with other circuit components. However, there are some challenges in the design of UWB

antennas, chief among them being interference. In the designated UWB operating band, several narrowband wireless systems also share parts of the spectrum and these include Worldwide Interoperability for Microwave Access (WiMAX: 3.3–3.6 GHz) and Wireless Local Area Network (WLAN: 5.15–5.35 GHz, 5.725–5.825 GHz) [4]. It is therefore necessary for an UWB antenna to be capable of rejecting the operating frequencies of these systems natively on the antenna, doing away with the need for an external band-stop filter in the receiver circuitry in the process.

Various techniques have been proposed in the UWB antenna to achieve band-notched performance. The most common approaches involve using slots, i.e., U-shape [5], square slot [6], quarter wavelength open-ended slots on the monopole and ground plane [7, 8, 9], and utilizing parasitic elements near the monopole [10], or near the feedline [11]. Other techniques involve the use of electromagnetic band gap

<sup>\*</sup> Corresponding author.

E-mail address: [smellis.coe@knust.edu.gh](mailto:smellis.coe@knust.edu.gh) (M.S. Ellis).

structures (EBGs) [12], defected ground structures (DGS) [13]. Recently, the split ring resonators SRR have also been introduced to achieved band notched functionality [14, 15].

In [14], a pair of split ring resonators is coupled to a coplanar waveguide fed monopole antenna to realize a single band notched within the UWB band. Even though this technique produced high gain suppression of -11dB, a required antenna size of  $50 \times 50 \text{ mm}^2$  is required. In [15], a multiband notched antenna is designed by loading the feedline of the antenna with three split ring resonators of different dimensions. A good gain suppression of -9.6, -12.7, and -4.3 dBi was realized at the notched frequencies. However, a large antenna of  $50 \times 70 \text{ mm}^2$  was required. Other techniques that employ reconfigurable antenna [16], and meandered lines [17] have also been proposed. In [16], a switch is employed inside a radiator of the antenna to achieve band notched switching by changing the slot length. The measured radiation patterns suffer from distortions due to the switch and length-fluctuations of the slot. In [17], four pair of meandered lines is used to realize multiple band notched properties. A high gain suppression of about 9 dBi is achieved but the antenna suffers from distorted radiation patterns.

Most of the aforementioned techniques have three main problems: (1) space limitation: such techniques require large gaps to be created per band-notch which it makes not feasible to use the same technique on the same antenna to create multiple band notches, and (2) band-notches created using these techniques have wide notch-widths, some exceeding a bandwidth of 2 GHz rejecting some useable frequencies in

the process. More importantly, (3) the filtering mechanism in terms of circuit analysis is not usually discussed. If there are, the circuits are drawn with little to no comprehensible explanation.

In this paper, a technique is proposed to realize a dual-band notched antenna that solves all the aforementioned problems. Additionally, a detailed explanation is provided on the filtering mechanism and the methodology can be replicated for other designs. Vertical quarter-wavelength stub(s) embedded in a closed slot on the feedline is employed to achieve band notched performances. Two antennas are proposed here: (1) using a single stub to achieve a narrow band-notch from 3.3 - 3.6 GHz, and (2) using two stubs in close proximity on a closed slot on the feedline to achieve dual band-notched properties, i.e., one narrow band (3.3–3.6 GHz) and a wider band-notch from (5.15–6 GHz). Compared with other designs, the proposed antennas do not employ the ground plane or radiator in achieving its multiple band notches and relatively accurate band-rejections. The proposed technique also uses very limited space, and achieves dual notch bands using only the feed line (see Figure 1).

## 2. Antenna design and implementation

The antennas are both printed on an FR4 substrate with a dielectric constant of 4.4, a thickness of 1.6 mm, and fed with a 50-Ω coaxial cable. The monopole and feedline are printed on top of the substrate and the ground plane is printed at the bottom. A slot is created on the feedline at a considerable distance above the attached SMA connector. In this work,

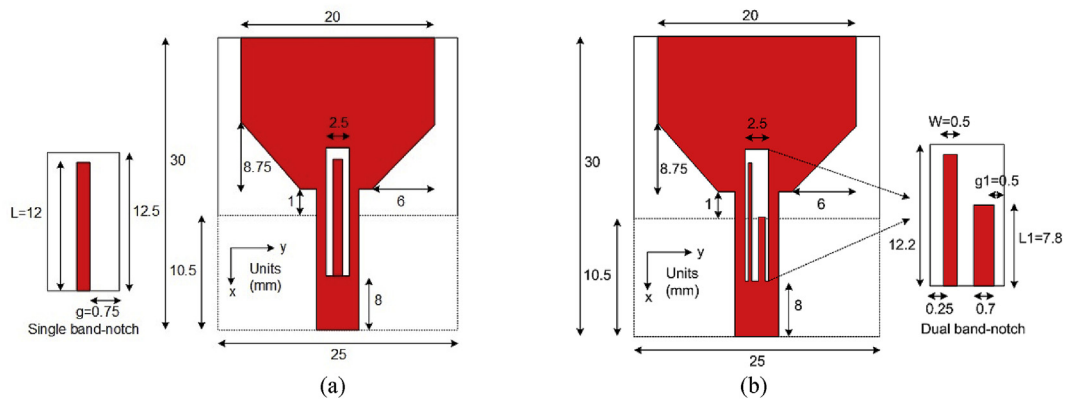


Figure 1. Geometry of the proposed (a) single band-notched antenna (b) dual band-notched antenna.

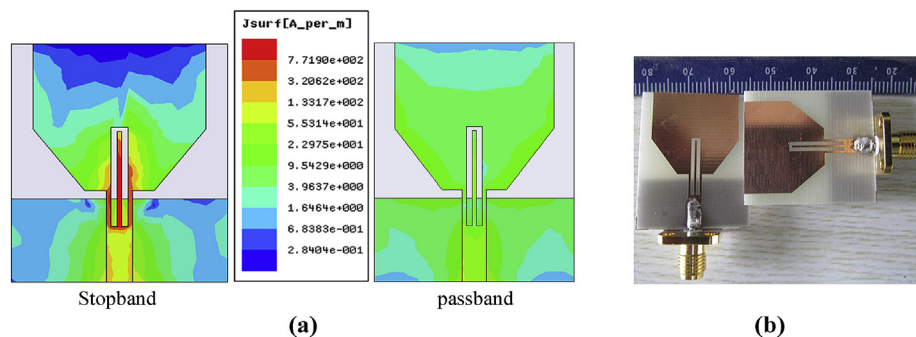


Figure 2. Simulation of proposed antenna showing (a) current distribution at the stopband and a passband, (b) Photograph of the fabricated prototype of the single notched band antenna.

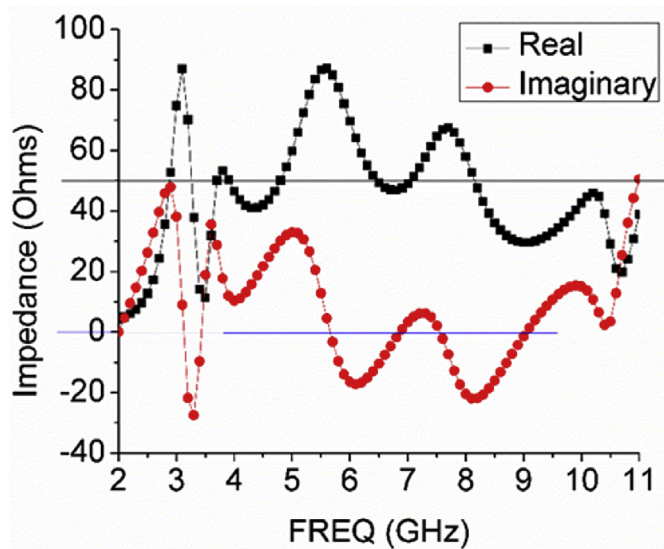


Figure 3. Impedance plot of the single band notched antenna drawn in HFSS (WiMAX notch in blue circle showing minimum real and imaginary impedances).

two quarter-wave strips are protruded from the feedline. The circuit representation is described in detail to provide information on realizing the stop bands. For a particular band notch, the total length  $L_{slot}$  of the stub is calculated using the following equations:

$$L_{stub} = \frac{\lambda_g}{4} = \frac{\lambda_0}{4\sqrt{\epsilon_{eff}}} = \left(\frac{c}{4f_{notch}}\right) \times \left(\frac{1}{\sqrt{\epsilon_{eff}}}\right) \tag{1}$$

$$\epsilon_{eff} = \left(\frac{\epsilon_r + 1}{2}\right) + \left(\frac{\epsilon_r - 1}{2}\right) \left(1 + \frac{12h}{w}\right)^{-1/2} \tag{2}$$

where  $\lambda_0$  is the free space wavelength,  $c$  is speed of light in free space,  $f_{notch}$  is the center notch frequency of the notched band,  $\epsilon_{eff}$  is the effective dielectric constant,  $\epsilon_r$  is the dielectric constant of the FR4 substrate,  $h$  is the height of the dielectric and  $w$  is the width of the feedline. The calculated values are used as starting values but are fully optimized in the simulation software for best results. However, the difference between the calculated and optimized value is negligible. The calculated value of  $L_{stub}$  for WiMAX was 13mm and the optimized value was 12mm. For WLAN, the calculated value of 8mm is achieved while an optimized value of 7.8mm is achieved.

### 3. Single band notch analysis & far field results

The single band-notched antenna is designed to mitigate interfering bands from the 3.3–3.6 GHz WiMAX band. It employs one vertical stub that acts as a band stop filter. The current distribution is shown in Figure 2(a). At the notched frequency, majority of the current is distributed along the strip and the edges of the feedline as shown in the figure. At this frequency, the currents on the strip and edges of the feedline move in opposite directions and therefore cancel each other's radiation. The radiation is therefore attenuated at that frequency and a

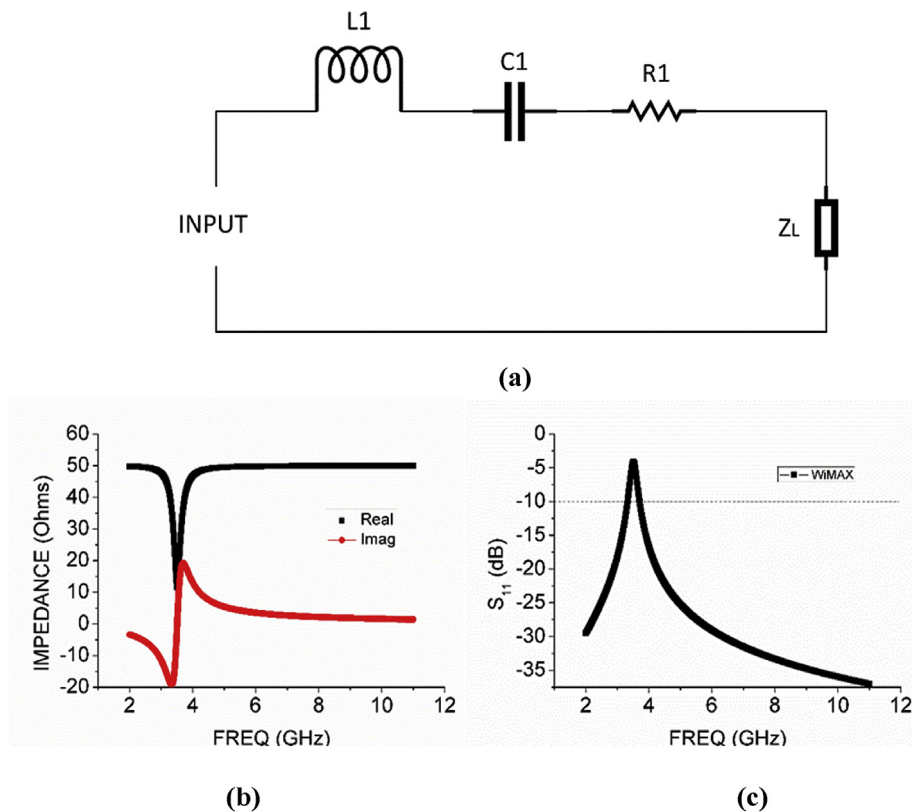


Figure 4. ADS results showing (a) equivalent RLC circuit at 3.5 GHz notch, (b) impedance of the RLC series filter, and (c)  $S_{11}$  of RLC circuit, and.

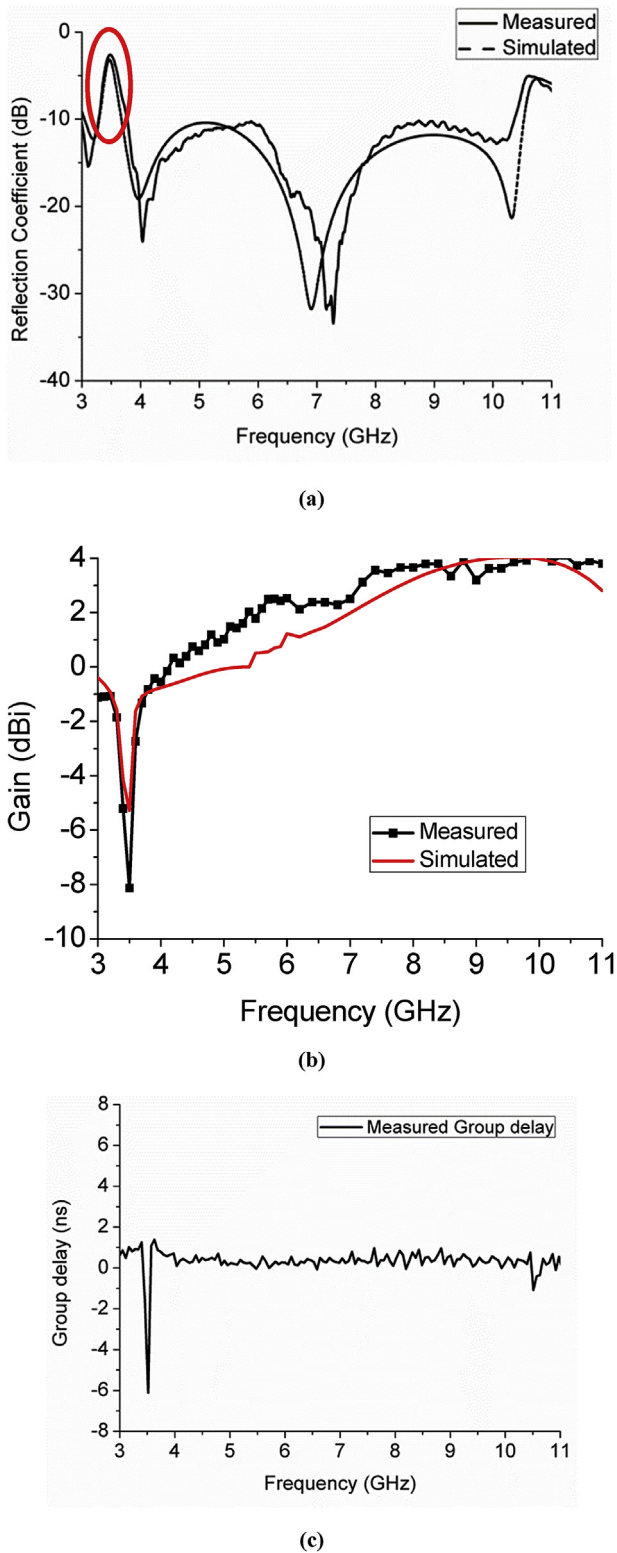


Figure 5. Far-field measurement results: (a)  $S_{11}$ , (b) gain, and (c) group delay.

notch is introduced. The proposed antenna was simulated with Ansys High Frequency Structure Simulator (HFSS).

The proposed antenna is fabricated as shown in Figure 2(b). The methodology of circuit representation of the antenna has been shown. To begin with, the impedance plot of the proposed To begin to comprehend how to design an equivalent circuit for this design, the simulated impedance plot of the proposed antenna was plotted in Ansys High Frequency Structure Simulator (HFSS) in Figure 3. It shows that the average value of the real component of the input impedance is around  $50 \Omega$  at the operating frequencies of the antenna (outside the filtered band) and the average imaginary component of the input impedance is  $0 \Omega$  at the operating frequencies (outside of the filtered band). It can be noticed that at the filtered band, the real and imaginary components of the impedance are both minimum. According to circuit theory, this impedance behavior is a characteristic of a series resonance circuit. Therefore, it is evident that the filter required to filter out the WiMAX band (3.3–3.6 GHz) has to be a series resonance circuit.

The next step is to calculate the values of the lumped circuit components for this series resonant circuit. Using the formulas in [18], the values of  $L$  and  $C$  can be calculated for this notch frequency using the formulas shown in Eqs. (3), (4), and (5). The calculated values of  $L_1$  and  $C_1$  were used as starting points ( $L_1 = 38.25\text{nH}$ ,  $C_1 = 2.13\text{pF}$ ) to design the equivalent circuit. The final optimized values were  $L_1 = 28\text{nF}$ ,  $C_1 = 0.0722\text{pF}$ . Discrepancies between the calculated values and the optimized values for the proposed antenna are noticed. This is because, other properties of the antenna, i.e., substrate, radiator, and feedline also affect the notch band, which are not considered in the equations above. The circuit was designed in Keysight's Advanced Design System (ADS) and the results are shown in Figure 3. It should be noted that a resistance,  $R_1$ , was included in the filter design to simulate the width of the notch. Hence a small value of  $R_1 = 15 \Omega$  was chosen to provide the desired notch width.

Fractional Bandwidth:

$$\Delta_1 = \frac{\omega_2 - \omega_1}{\omega_0} = \frac{3.7 - 3.3}{3.5} = 0.1142857 \quad (3)$$

Series L and C:

$$L_1 = \frac{Z_0 * L'_1}{\omega_0 * \Delta_1} \text{ where } L'_1 = 0.3052 \quad (4)$$

$$C_1 = \frac{\Delta_1}{Z_0 * L'_1 * \omega_0} \text{ where } C'_1 = 1 \quad (5)$$

where  $Z_0 = 50\Omega$ , where  $L'_1 = 0.3052$  and  $C'_1 = 1$  are the element values as specified in [12].

The circuit is now drawn using the optimized values of the components as shown in Figure 4(c). The series combination of the circuit is then drawn with the optimized values of the calculated components as shown in Figure 4(a). The impedance and reflection coefficient of the circuit are plotted in ADS as well. It can be seen that they match the desired results of the HFSS design shown in Figures 3 and 5(a), respectively. This therefore confirms that our circuit design is accurate and reflects the results realized in HFSS.

The measured reflection coefficients, gain and group delay are plotted in Figures 5(a), 5(b) and 5(c) respectively. The  $S_{11}$  is measured with an Agilent E8363C Performance Network Analyzer and the far field

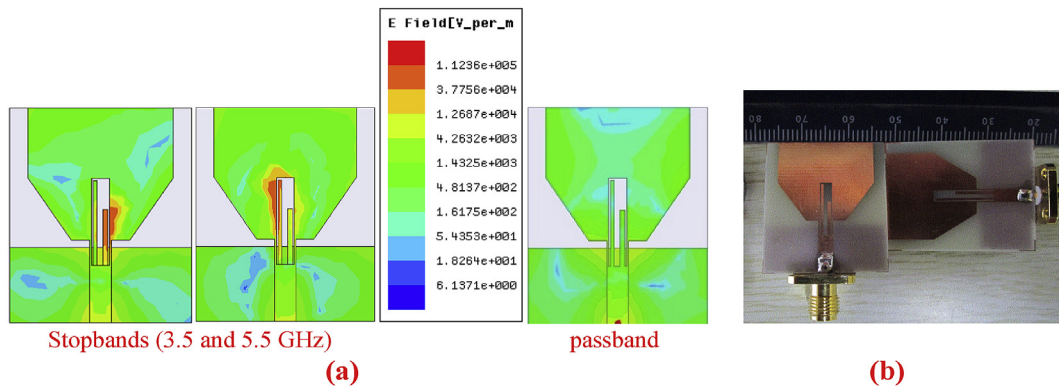


Figure 6. Simulation of proposed antenna showing (a) current distribution at the stopband and a passband, (b) Photograph of the fabricated prototype of the dual band notched antenna.

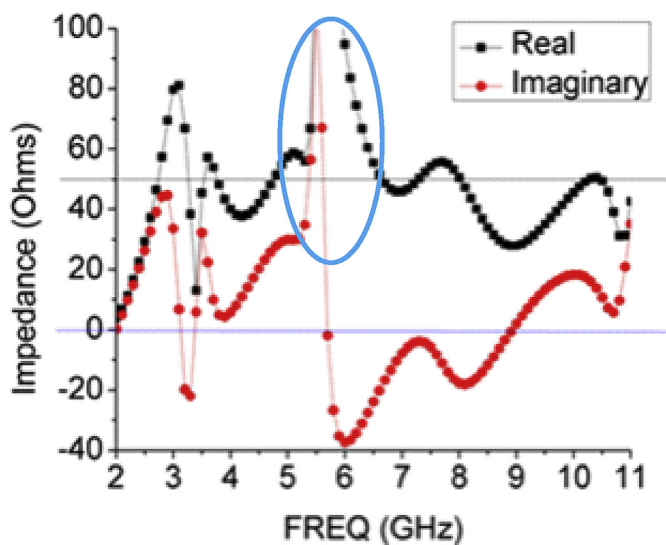


Figure 7. Simulated impedance plot of the dual band notched antenna drawn in HFSS (WLAN notch in blue circle showing maximum real and imaginary impedances).

measurements are done with a Pyramidal Anechoic Chamber measurement system. It can be noticed that an ultra-wideband impedance bandwidth is achieved from 3 – 10.6 GHz ( $S_{11} < -10$  dB) with a band notch at 3.3–3.65 GHz. This shows that the proposed technique can be used to accurately reject a narrow frequency band. Simulated and measured results also agree well. Slight discrepancies may be due to the attached SMA and fabrication imperfections. The measured and simulated peak gain also shows that an average peak gain of 2 dBi is achieved within the UWB band with a gain suppression of about 7 dBi at the notch band. The group delay also shows a constant delay between 0.5 – 1 ns within the desired UWB band but with a large delay at the notched band, as expected.

#### 4. Dual band notch analysis & far field results

Next, the second filtered band is introduced which is the WLAN band from 5.15 – 6 GHz. The current distribution of the antenna with

dual band notches is shown in Figure 6. At the notched frequency, majority of the current is distributed along the strip and the edges of the feedline as shown in figure 6(a) and (b) at both frequencies. At these frequencies, the currents on the strip and edges of the feedline move in opposite directions and therefore cancel each other's radiation. The radiation is therefore attenuated at those frequencies and the band notches are introduced. This is achieved when the strip inside the slot is designed according to Eqs. (1) and (2). At the passbands however, no such phenomenon is realized. A uniform distribution is seen.

The input impedance plot in Figure 7 shows that the average values of the real and imaginary components of the input impedance are both maximum at the filtered frequency. Based on circuit theory, this is a characteristic of a parallel resonant circuit. The values of  $L_2$  and  $C_2$  are calculated using Eqs. (6), (7) and (8) below.

Fractional bandwidth:

$$\Delta_2 = \frac{\omega_2 - \omega_1}{\omega_0} = \frac{6.1 - 5.15}{5.625} = 0.1688889 \quad (6)$$

Series L and C:

$$L_2 = \frac{\Delta_2 * Z_0}{\omega_0 * C'_2} \quad (7)$$

$$C_2 = \frac{C'_2}{Z_0 * \omega_0 * \Delta_2} \quad (8)$$

where  $Z_0 = 50\Omega$ , and  $C'_2 = 1$  is element value as specified in [18].

The design is implemented in ADS and values are optimized for best results. To find the starting values, Eqs. (6), (7) and (8) are used and the calculated values of  $L_2$  and  $C_2$  are found as 0.239nH and 3.33pF. The values are then optimized for our proposed design and the final values are given as  $L_2 = 0.148$ nH and  $C_2 = 5.70$ pF. Again, a resistance,  $R_2$ , was included in the filter design to adjust the width of the notch. Hence, a value of  $R_2 = 500 \Omega$  was chosen to provide the best notch width. Figure 8(a) shows the complete circuit representation that shows the WLAN and WiMAX filters, representing the band-notched techniques implemented on the antenna.

The impedance and reflection coefficient of the circuit are plotted in ADS. It can be seen from Figure 8 that they match the desired results of the HFSS design shown in Figure 7 and Figure 9(a), respectively. This therefore confirms that our circuit design is accurate and reflects the results realized in HFSS.

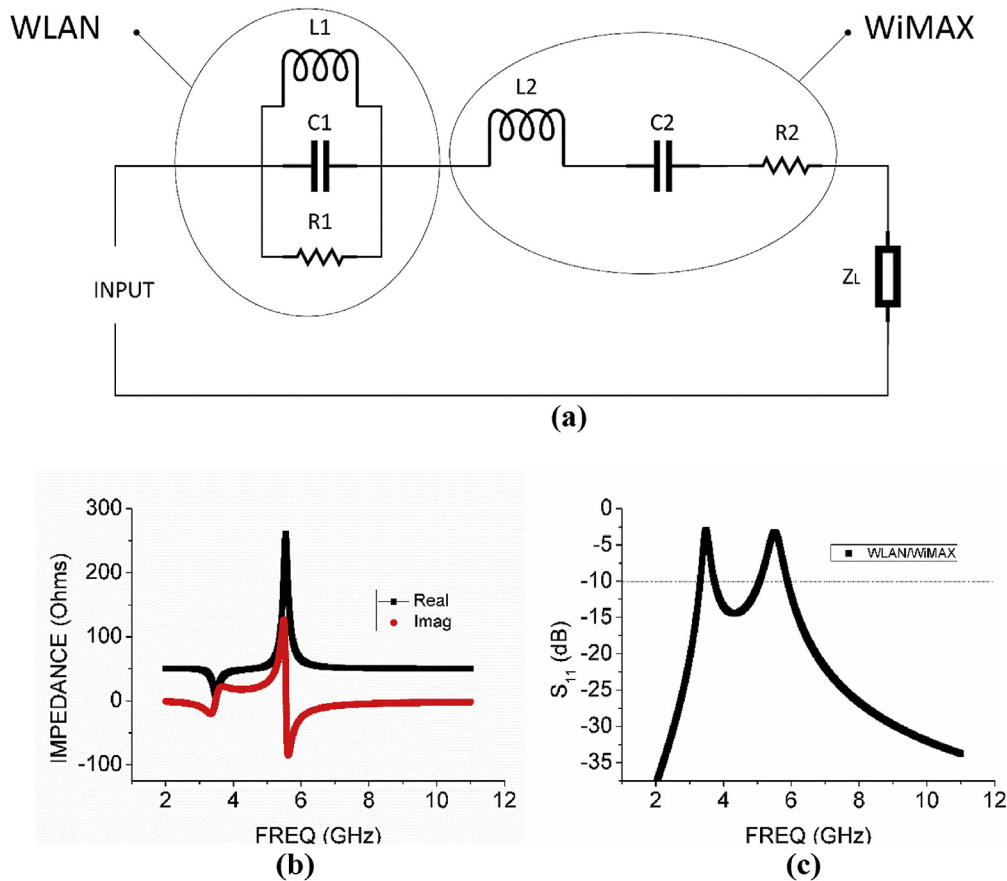


Figure 8. ADS results showing (a) equivalent circuit of proposed dual-notched antenna (b) impedance, and (c) S<sub>11</sub>.

The measured results are shown in Figure 9. Satisfactory agreement is achieved between the simulations and measurements at the two notch frequencies. Figure 9(a) shows that at the lower band WiMAX band, the notch for the simulated result occurs between 3.25 - 3.6 GHz while the measured results occurs between 3.25 - 3.8 GHz. At the high frequency band, a perfect match between the simulated and measured results is achieved from 5.15 - 6.1 GHz, showing accuracy in the proposed technique. It can be noticed that there is a slight shift in the lower frequency notch in the proposed dual notch antenna compared to the single notched antenna. This is possibly due to the proximity of the second strip to the first strip which may introduce some coupling. Nonetheless, the difference is not significant. There is also some discrepancy between the measured and simulated results around 8-9 GHz. This can be attributed to the attached SMA connector. Due to the small size of the ground plane of the antenna, the antenna's radiating performance which is dependent on the ground plane could be affected when the SMA is attached [19, 20, 21]. The simulated and measured gain of the proposed dual notch antenna is shown in Figure 9 (b). It shows 7 dBi gain suppression at the lower notch band and 5 dBi gain suppression at the higher notch band. The group delay is plotted in Figure 9(c). Group delay is critical in UWB antennas as it represents the degree of distortion in the pulse signal

from the transmitter to the receiver. For good pulse transmission, the group delay should be almost constant (between 0 - 1 ns). As noticed, the group delay ripple is less than 1ns across the entire bandwidth except at the notched bands where they depict significant delays of -4ns and -5ns in the WiMAX and WLAN bands, respectively. This shows that the proposed antenna is suitable for UWB transmission and also confirms the effectiveness of the proposed technique in filtering these unwanted bands. The efficiency of the antenna with and without the band-notched technique is plotted in Figure 9(d). It shows that the efficiency drops tremendously at the notched frequencies. This is in agreement with the gain and group delay plots in Figures 9 (b) and (c).

The proposed antenna is printed on the *xoy*- plane. Therefore, the E-plane (*xoy*,  $\theta = -90^\circ$ ) and H-plane (*yo<sub>z</sub>*,  $\varphi = 90^\circ$ ) radiation patterns are plotted at 3.1 GHz, 6.2 GHz, and 8.5 GHz. As shown in Figure 9(e), it can be noticed that the E-plane radiation patterns depict a quasi-omnidirectional radiation pattern and the H-plane depicts an omnidirectional radiation pattern, with low cross-polarization.

The 3D polar plots are shown in Figure 10. It shows that at the passbands, an appreciable gain is realized as expected. But at the notched bands, the gain greatly depreciates. A gain of 4.6 dBi and 6.8 dBi are realized at the chosen passbands while gains of -3.5 dBi and

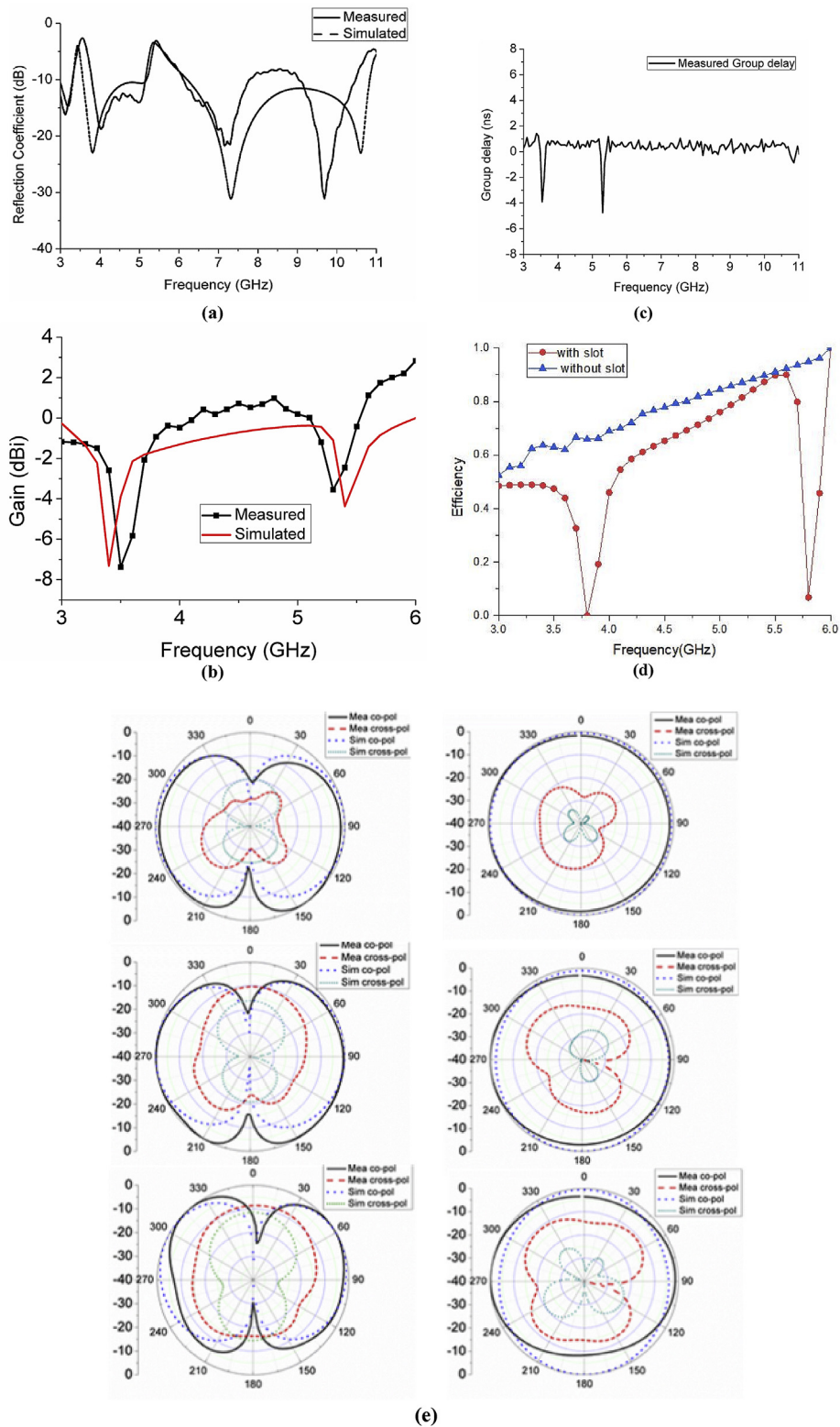


Figure 9. Measured and simulated (a)  $S_{11}$  (b) Gain (c) Group delay (d) E-plane (left), and H-plane (right) radiation patterns at 3.1 GHz (top), 6.2 GHz (middle), and 8.5GHz (bottom).

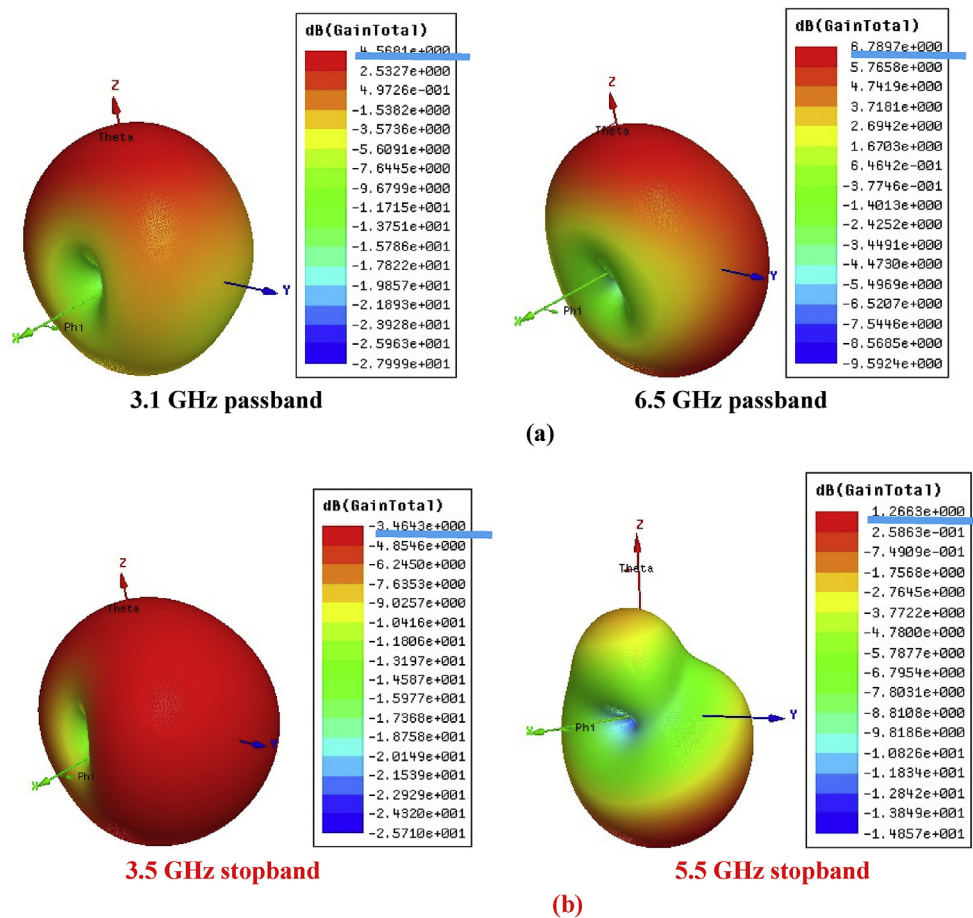


Figure 10. Effect of band-notched on radiation pattern and gain (a) passbands (b) stopbands.

-3.8 dBi are achieved at the notched bands, at 3.5 GHz and 5.5 GHz, respectively.

**5. Conclusion**

A technique of using vertical stubs protruding from the feedline to achieve single and dual band-notches in a UWB antenna is proposed. The simulated and the experimental results show that the proposed technique solves the problems associated with band-notch modules; 1) space reduction of the proposed technique and 2) accurate narrow band rejection. More importantly, (3) a step by step approach on circuit analysis has been presented. The methodology can be replicated for single band and multiple bands as demonstrated. Also, it can be replicated to explain other band notched antenna designs. This solves the third problem: lack of detailed and replicable understanding the filtering technique, which is lacking in similar works.

**Declarations**

*Author contribution statement*

Mubarak Sani Ellis: Conceived and designed the experiments; Performed the experiments; Wrote the paper.

Philip Arthur: Performed the experiments; Analyzed and interpreted the data.

Abdul Rahman Ahmed & Jerry John Kponyo: Analyzed and interpreted the data.

Benedicta Andoh-Mensah & Bob John: Contributed reagents, materials, analysis tools or data.

*Funding statement*

This research did not receive any specific grant from funding agencies in the public, commercial, or not-for-profit sectors.

*Data availability statement*

No data was used for the research described in the article.

*Declaration of interests statement*

The authors declare no conflict of interest.

*Additional information*

No additional information is available for this paper.

**References**

- [1] P. Li, J. Liang, X.D. Chen, Study of printed elliptical/circular slot antennas for ultrawideband Applications, *IEEE Trans. Antenn. Propag.* 56 (2006) 1675, 1675.
- [2] D. Singh, V.M. Srivastava, Dual resonance shorted stub circular rings metamaterial absorber, *AEU-Int. J. Electron. Commun.* 83 (2018) 58–66.
- [3] H.G. Schantz, A brief history of UWB antennas, *IEEE A&E Syst. Mag.* 19 (4) (2004) 22–26.
- [4] M. Majidzadeh, C. Ghobadi, J. Nourinia, Novel single layer reconfigurable frequency selective surface with UWB and multi-band modes of operation, *AEU-Int. J. Electron. Commun.* 70 (2016) 151–161.
- [5] H.S. Mewara, D. Jhanwar, M.M. Sharma, J.K. Deegwal, A printed monopole ellipsoidal UWB antenna with four band rejection characteristics, *AEU-Int. J. Electron. Commun.* 83 (2017) 222–232.

- [6] R. Zaker, C. Ghobadi, J. Nourinia, Novel modified UWB planar monopole antenna with variable frequency band-notched function, *IEEE Antenn. Wireless Propag.* 7 (2008) 112–114.
- [7] A.M. Abbosh, M.E. Bialkowski, J. Mazierska, M.V. Jacob, A planar UWB antenna with signal rejection capability in the 4–6 GHz band, *IEEE Microw. Wireless Compon. Lett.* 16 (5) (2006) 278–280.
- [8] Z.A. Zheng, Q.X. Chu, Z.H. Tu, Compact band-rejected ultrawideband slot antennas inserting with  $\lambda/2$  and  $\lambda/4$  resonators, *IEEE Trans. Antenn. Propag.* 59 (2) (2011) 390–397.
- [9] I.J. Yoon, H. Kim, H.K. Yoon, Y.J. Yoon, Y.H. Kim, Ultrawideband tapered slot antenna with band cutoff characteristics, *Electron. Lett.* 41 (11) (2005) 629–630.
- [10] D. Yadav, M.P. Abegaonkar, S.K. Koul, V. Tiwari, D. Bhatnagar, A compact dual band-notched UWB circular monopole antenna with parasitic resonators, *AEU-Int. J. Electron. Commun.* 84 (2017) 313–320.
- [11] A. Yadav, S. Agrawal, R.P. Yadav, SRR and S-shape slot loaded triple band notched UWB antenna, *AEU-Int. J. Electron. Commun.* 79 (2017) 192–198.
- [12] L. Peng, C.-L. Ruan, UWB band-notched monopole antenna design using electromagnetic bandgap structures, *IEEE Trans. Antenn. Propag.* 59 (4) (2011) 1074–1081.
- [13] A. Nouri, G.R. Dadashzadeh, A compact UWB band-notched printed monopole antenna with defected ground structure, *IEEE Antenn. Wireless Propag. Lett.* 10 (2011) 1178–1184.
- [14] J.Y. Siddiqui, C. Saha, Y.M.M. Antar, Compact SRR loaded UWB circular monopole antenna with frequency notch characteristics, *IEEE Trans. Antenn. Propag.* 62 (8) (2014) 4015–4020.
- [15] L.A. Shaik, C. Saha, J.Y. Siddiqui, Y.M.M. Antar, Ultra-wideband monopole antenna for multiband and wideband frequency notch and narrowband applications, *IET Microw. Antennas Propag.* 10 (11) (2016) 1204–1211.
- [16] M.A. Abdallah, A.A. Ibrahim, A. Boutejdar, Resonator switching techniques for notched ultrawideband antenna in wireless applications, *IET Microw., Antennas Propag.* 9 (13) (2015) 1641–1677.
- [17] Y.F. Weng, S.W. Cheung, T.I. Yuk, Design of multiple band-notch using meander lines for compact ultrawide band antennas, *IET Microw., Antennas Propag.* 6 (8) (2012) 908–914.
- [18] D.C. Vaghela, A.K. Sisodia, N.M. Prabhakar, Design, simulation and development of bandpass filter at 2.5 GHz, *Int. J. Exp. Diabetes Res.* 3 (Issue 2) (2015) 1202–1209.
- [19] M.S. Ellis, Z. Zhao, J. Wu, Z. Nie, Q.H. Liu, Small planar monopole ultra-wideband Antenna with reduced ground plane effect, *IET Microw., Antennas Propag.* 9 (10) (2015) 1028–1034.
- [20] K. Vyas, R.P. Yadav, Planar suspended line technique based UWB-MIMO antenna having dual-band notching characteristics, *Int. J. Microwave Wireless Tech.* 13 (6) (2021) 614–623.
- [21] K. Kumar, S. Dwari, M.K. Mandal, An ultra-wideband surface wave antenna with reduced ground plane effects, *Int. J. RF Microw. Computer-Aided Eng.* 31 (11) (2021), e22819.